Dynamin-dependent endocytosis of ionotropic glutamate receptors

Reed C. Carroll*†‡, Eric C. Beattie*†, Houhui Xia*‡, Christian Lüscher§¶, Yoram Altschuler‖, Roger A. Nicoll§, Robert C. Malenka*‡***, and Mark von Zastrow*§††**

Departments of *Psychiatry, §Cellular and Molecular Pharmacology, ‖Anatomy, and **Physiology, University of California, San Francisco, CA 94143

Contributed by Roger A. Nicoll, September 24, 1999

Little is known about the mechanisms that regulate the number of ionotropic glutamate receptors present at excitatory synapses. Herein, we show that GluR1-containing α-amino-3-hydroxy-5-methyl-4-isoxazolepropionic acid (AMPA) receptors (AMPARs) are removed from the postsynaptic plasma membrane of cultured hippocampal neurons by rapid, ligand-induced endocytosis. Although endocytosis of AMPARs can be induced by high concentrations of AMPA without concomitant activation of *N*-methyl-D-aspartate (NMDA) receptors (NMDARs), NMDAR activation is required for detectable endocytosis induced by synaptically released glutamate. Activated AMPARs colocalize with AP2, a marker of endocytic coated pits, and endocytosis of AMPARs is blocked by biochemical inhibition of clathrin-coated pit function or overexpression of a dominant-negative mutant form of dynamin. These results establish that ionotropic receptors are regulated by dynamin-dependent endocytosis and suggest an important role of endocytic membrane trafficking in the postsynaptic modulation of neurotransmission.

Fast excitatory synaptic transmission in the mammalian central nervous system is mediated primarily by α-amino-3-hydroxy-5-methyl-4-isoxazolepropionic acid (AMPA)-type and *N*-methyl-D-aspartate (NMDA)-type ionotropic glutamate receptors, which are coexpressed at many synapses and subserve distinct physiological functions in synaptic transmission (1–3). Although the vast majority of excitatory synapses in the hippocampus expresses functional NMDA receptors (NMDARs), electrophysiological and anatomical data suggest that the number of AMPA receptors (AMPARs) expressed at individual synapses on CA1 pyramidal cells is highly variable (4–8). Furthermore, recent evidence suggests that the surface expression of AMPARs at individual synapses is not fixed but is dynamically regulated by neuronal activity (2, 9–12). This activity-dependent regulation of the synaptic expression of AMPARs may contribute to the changes in synaptic strength that occur during NMDAR-dependent long-term potentiation and long-term depression (11, 12).

Surprisingly, little is known about the detailed molecular mechanisms that regulate the number of AMPARs at excitatory synapses. Previously, we showed a pronounced redistribution of AMPARs away from synaptic sites within minutes after the triggering of long-term depression (12) or pharmacological activation of AMPARs (13). Herein, we show that this process is mediated by dynamin-dependent endocytosis and identify a role of NMDAR activation in promoting AMPAR endocytosis under physiological conditions.

Materials and Methods

Cell Culture and Immunocytochemistry. Hippocampal cultures were prepared as described (12, 13) and were used for experimentation at 2–3 weeks after plating. Surface AMPARs were stained with an antibody recognizing an extracellular epitope (amino acids 271–285) of the rat GluR1 subunit (Oncogene Research). Before treatment, antibody (5 μg/ml) was applied to live cells for 15 min at 37°C in conditioned cell medium. Cells were then briefly washed and returned to medium for agonist treatment. Tetrodotoxin (1 μM) was included for all treatments, and 50 μM D-2-amino-5-phosphonovaleric acid (D-APV) was present for experiments in which 100 μM AMPA was applied for 15 min. To visualize surface and internalized receptors in the same specimens selectively (Fig. 1*A*), antibody-labeled cells were fixed with 4% paraformaldehyde in PBS immediately after treatment. Fixed cells were then washed with PBS and blocked in Tris-buffered saline (TBS) supplemented with 2% (vol/vol) BSA but no detergent (to prevent permeabilization). Specimens were then incubated with donkey anti-rabbit FITC conjugate (Jackson ImmunoResearch; 1:300 dilution) for 1 h to detect specifically antibody-labeled receptors in the plasma membrane. After extensive washing in PBS (to remove residual secondary antibody), cells were permeabilized with 0.1% Triton X-100, and internal receptors were detected by incubation with donkey anti-rabbit Cy3 conjugate for 1 h (Jackson ImmunoResearch; 1:300 dilution).

In acid-stripping experiments, antibody-labeled cells were chilled immediately after agonist treatment by using ice-cold TBS. Then, intact cells were exposed to 0.5 M NaCl/0.2 M acetic acid for 4 min on ice. This procedure selectively strips bound antibody from the cell surface and leaves intracellular antibody–receptor complexes intact (14, 15). After acid stripping, cells were washed three times with ice-cold TBS and fixed in paraformaldehyde as described above. After permeabilization with 0.1% Triton X-100 in TBS containing 2% (vol/vol) BSA, acid-resistant immunoreactivity representing internalized receptors was detected by using donkey anti-rabbit Cy3 conjugate. Epifluorescence microscopy was carried out by using a Nikon ×60 NA1.4 objective and FITC and Cy3 filter sets (Omega Optical). Images were captured with a cooled CCD camera, and minimal bleed-through between channels was confirmed as described (9, 13).

The time course of internalization was determined by adding agonist to antibody-labeled cells for the indicated periods of time, after which cells were chilled and subjected to acid stripping to visualize internalized antibody–receptor complexes. To examine the effects of a brief application of agonist, cells were incubated in AMPA or glutamate for 1 or 5 min, and then agonist was removed rapidly by washing with fresh culture medium supplemented with the AMPAR antagonist CNQX (50 μM) and/or the NMDAR antagonist D-APV (50 μM). Cells were

Abbreviations: AMPA, α-amino-3-hydroxy-5-methyl-4-isoxazolepropionic acid; AMPAR, AMPA receptor; NMDA, *N*-methyl-D-aspartate; NMDAR, NMDA receptor; D-APV, D-2-amino-5-phosphonovaleric acid; CNQX, 6-cyano-7-nitroquinoxaline-2,3-dione; HA, hemagglutinin; TBS, Tris-buffered saline.

†R.C.C. and E.C.B. contributed equally to this work.

‡Present address: Nancy Friend Pritzker Laboratory, Department of Psychiatry and Behavioral Sciences, Stanford University School of Medicine, Stanford, CA 94304.

¶Present address: Departments de Physiologie et Pharmacologie Fondamentale, Service de Neurologie, Université de Geneve, 1211 Geneva 4, Switzerland.

††To whom reprint requests should be addressed. E-mail: zastrow@itsa.ucsf.edu.

The publication costs of this article were defrayed in part by page charge payment. This article must therefore be hereby marked "*advertisement*" in accordance with 18 U.S.C. §1734 solely to indicate this fact.

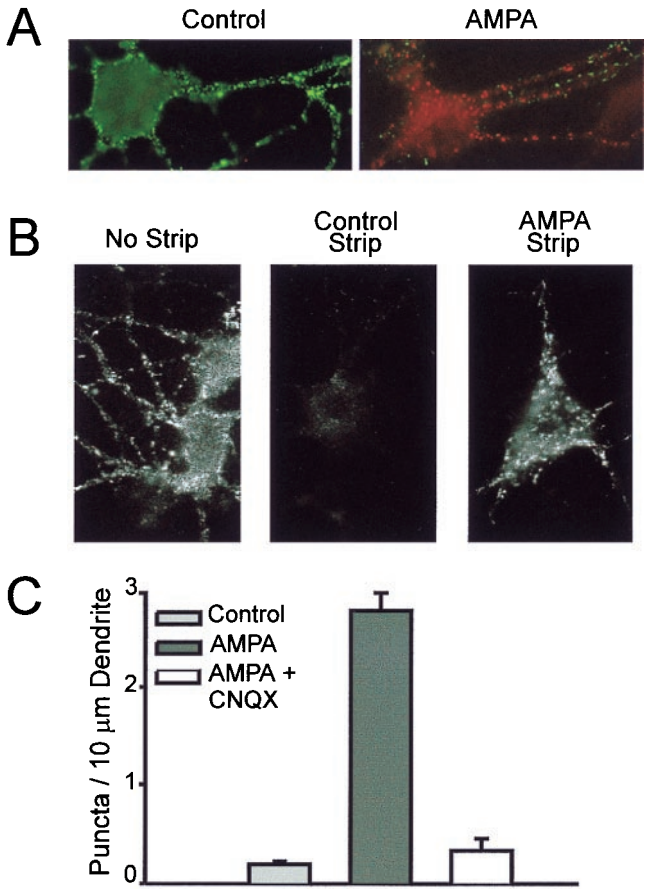

Fig. 1. AMPARs are internalized after exposure to AMPA. (*A*) Living cells were labeled for surface AMPARs before treatment. After agonist application, surface receptors were detected with secondary antibodies on nonpermeabilized cells. Cells were then permeabilized, and internalized receptors were detected by using a secondary antibody with a different fluorescent conjugate. In an untreated cell (*Left*), AMPARs were primarily at the cell surface (green) with minimal internalized receptor immunoreactivity (red). Exposure to 100 μM AMPA for 15 min (*Right*) caused a dramatic increase in the amount of internalized AMPARs (red) along with a concomitant reduction in the amount of surface AMPAR staining (green). (*B*) Antibody-bound AMPARs internalized from the surface during agonist treatment are visualized exclusively by acid stripping antibodies from remaining surface AMPARs. In untreated, unstripped cells (*Left*), surface AMPARs were visualized in numerous puncta. After acid stripping of untreated cells (*Center*), labeling of surface AMPARs was almost abolished. After exposure of cells to 100 μM AMPA for 15 min, prominent staining of intracellular AMPAR puncta was apparent (*Right*), reflecting internalization of antibody-labeled AMPARs. (*C*) Quantitation of the acid-stripping assay in multiple specimens. Ordinate is mean number of internalized (acid-resistant) AMPAR puncta visualized per 10 μM dendrite for untreated cells (control), AMPA-treated cells (AMPA), and cells incubated for 15 min in the presence of 100 μM AMPA + 50 μM 6-cyano-7-nitroquinoxaline-2,3-dione (CNQX).

incubated further until 15 min after initial application of agonist. The effects of KCl-mediated depolarization were examined by exposing antibody-labeled cells to culture medium containing 30 mM KCl for 1 min, replacing with normal medium, continuing incubation for 15 min, chilling cells, and performing the acid-strip procedure described above.

To examine colocalization of ligand-activated AMPARs with the clathrin-associated endocytic coat protein AP2, antibodies to GluR1 and AP2 (AP.6 mouse monoclonal antibody, a gift of Frances Brodsky, University of California, San Francisco) were used and detected by goat anti-rabbit FITC conjugate and donkey anti-mouse Cy3 conjugate (Jackson ImmunoResearch), respectively. Specimens were analyzed by collecting optical sections with an MRC 1000 laser-scanning confocal microscope (Bio-Rad) equipped with a krypton/argon laser interfaced to a Zeiss Axiovert microscope (Zeiss ×100 NA1.3 objective). Control experiments (with single-labeled specimens) confirmed negligible bleed-through between channels.

Inhibition of Endocytosis. Cultures were preincubated in culture medium supplemented with 350 mM sucrose for 10 min to inhibit endocytosis mediated by clathrin-coated pits (16), and then anti-GluR1 antibody was added to the culture medium for an additional 15 min. Cells then were subjected to the agonist treatments and processed for immunocytochemical detection of AMPAR internalization by using the acid-strip procedure.

To examine the role of dynamin, cultures were exposed to replication-defective adenovirus vectors encoding hemagglutinin (HA)-tagged wild-type or K44A mutant dynamin-2 for 2 h at 15 plaque-forming units per cell as described (17). Cells were then allowed to recover for 24 h in control medium, at which point AMPAR internalization was examined by using the acid-strip assay. Neurons expressing recombinant dynamin were identified after acid stripping and permeabilization by using staining with mouse anti-HA followed by donkey anti-mouse FITC and dual channel epifluorescence microscopy. Typically 40–50% of neurons were transfected under these conditions.

Quantitative Analysis of Microscopic Data. Acid-resistant AMPAR puncta were visualized by using dual-color fluorescence microscopy, as described above. Dynamin-expressing neurons were chosen randomly, and acid-resistant AMPAR immunoreactivity was imaged by using a cooled CCD camera (Princeton Instruments). All specimens were imaged under identical conditions and images were normalized with the same "linear lookup" table by using IPLAB SPECTRUM software (Signal Analytics, Vienna, VA) before analysis for number of internalized (acid-resistant) AMPAR puncta. The level of internalized AMPAR immunoreactivity in untreated cells was de-

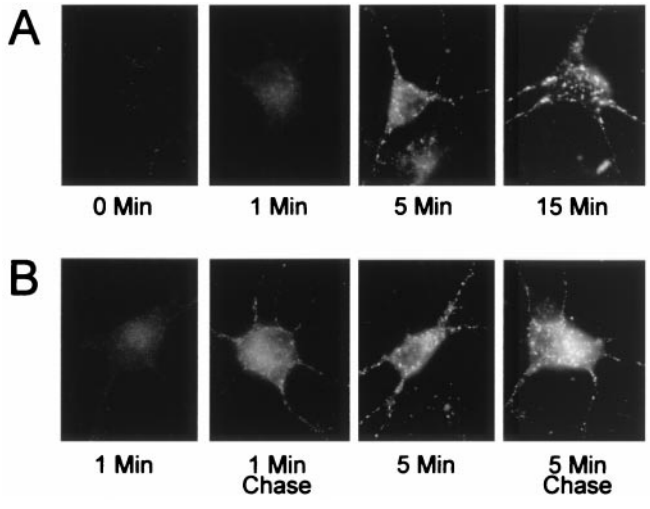

Fig. 2. Time course of ligand-induced internalization of AMPARs. (*A*) Cultured neurons were surface labeled with anti-GluR1 antibody, treated with 100 μM AMPA for 0, 1, 5, and 15 min, then immediately chilled on ice, and analyzed for AMPAR internalization by using the acid-strip procedure. Minimal AMPAR internalization is detected until 5 min of AMPA exposure. (*B*) Internalization of AMPARs can be initiated within 1 min after ligand-induced activation. Cells were incubated in the presence of 100 μM AMPA for 1 min or 5 min and then analyzed by using the acid-strip procedure either immediately (first and third panels) or after agonist washout and chase incubation in the presence of CNQX and D-APV for a total of 15 min (second and fourth panels).

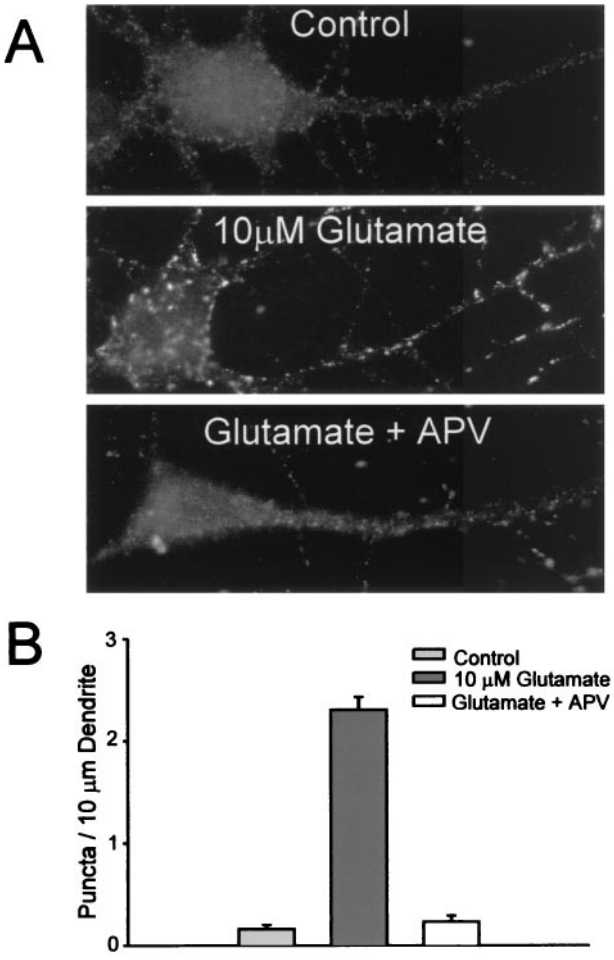

Fig. 3. Internalization of AMPARs is induced by glutamate and facilitated by NMDAR activation. (*A*) Incubation of cells with 10 μM glutamate for 1 min followed by chase incubation in the presence of CNQX and D-APV (APV) induced readily detectable internalization of AMPARs (*Middle*) compared with untreated cells (*Top*). Inclusion of D-APV (50 μM) in the pulse incubation strongly inhibited this process (*Bottom*). (*B*) Quantitation of the number of internalized AMPAR puncta under these conditions (n = 25 for each group).

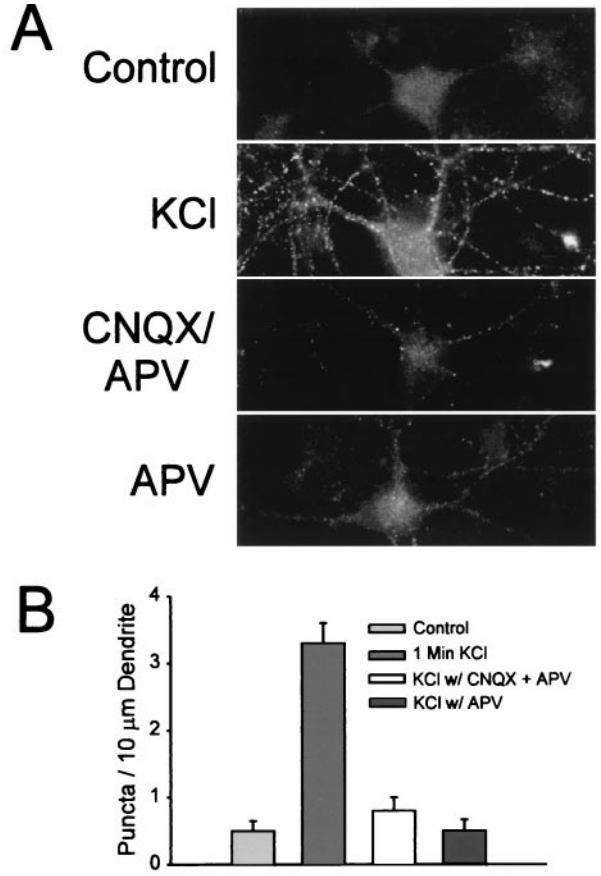

Fig. 4. Internalization of AMPARs induced by synaptically released glutamate. (*A*) Application of KCl (30 mM for 1 min) followed by 14 min chase incubation in normal medium caused significant internalization of AMPARs (compare top two panels). Blockade of glutamate receptors with CNQX and D-APV strongly inhibited this process, confirming that KCl-induced internalization of AMPARs is mediated by endogenously released glutamate binding to receptors. AMPAR internalization induced by KCl was also strongly inhibited by the NMDAR-specific antagonist D-APV. (*B*) Quantitation of AMPAR internalization in the absence and presence of receptor antagonists (n = 23 for each group).

fined as background. This definition facilitated detection of the regulated component of AMPAR internalization but would reduce detection of constitutive internalization. For all analyses, the investigator had no knowledge of the treatment history of the cells. Puncta were identified as discrete regions of immunoreactivity greater than 2-fold higher in intensity than the image background. Out-of-focus and extended, nondiscrete regions of staining were excluded from the quantitation. For all experiments, control and stimulated slips were obtained from the same culture preparation and were processed in parallel for immunofluorescence. For all immunocytochemical experiments, "n" refers to the number of microscopic fields (each containing 1–3 neurons) of dendritic processes analyzed. Each experimental manipulation was performed 3–6 times. For most analyses, puncta in well defined proximal dendrites were counted. In experiments with recombinant dynamin, soma and immediately proximal dendrites were counted, because these regions gave the clearest signal for HA-tagged dynamin. The average somatic area of cells counted under each condition was the same. Error bars in figures represent SEM.

Results

Rapid Ligand-Induced Internalization of AMPARs. We used an antibody recognizing an extracellular epitope of GluR1 to visualize specifically the subcellular distribution of endogenously expressed AMPARs in cultured hippocampal neurons. The specificity of this antibody was confirmed in control experiments that showed specific detection of recombinant GluR1 in transfected HEK 293 cells and blockade of endogenous GluR1 immunoreactivity in hippocampal neurons by a synthetic peptide comprising the antigenic epitope (not shown). Surface-associated AMPARs (Fig. 1*A Left*, green) were localized in a punctate pattern, 70–80% of which colocalized with synaptophysin immunoreactivity (not shown; ref. 12). Internalized AMPAR immunoreactivity, measured after cell permeabilization (see *Materials and Methods* for details), was almost undetectable in these same untreated cells (Fig. 1*A Left*, red). After exposure of cells to 100 μM AMPA for 15 min, a pronounced increase in internalized AMPAR immunoreactivity was observed (Fig. 1*A Right*, red) that was associated with a concomitant decrease in the staining of surface AMPAR puncta (Fig. 1*A Right*, green).

We next applied a method to detect specifically endocytosis of AMPARs by visualizing receptor-mediated endocytosis of antibody from the culture medium (18) by using an acid-stripping procedure (14, 15) to dissociate antibody from surface-accessible receptors and specifically retain labeling of internalized receptors that are resistant to acid stripping (19). Acid stripping

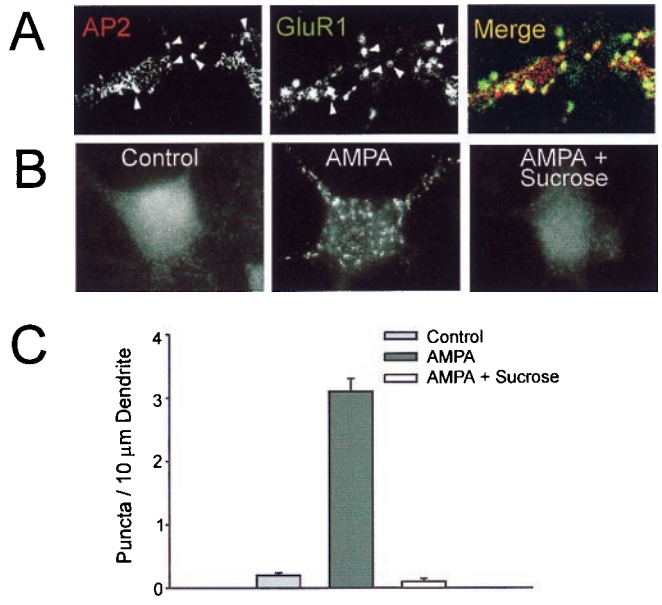

Fig. 5. Evidence for role of clathrin-coated pits in AMPAR endocytosis. (*A*) After surface labeling AMPARs and brief application of AMPA cells were fixed and permeabilized, and antibody-labeled AMPARs and immunoreactive AP2 were detected in the same specimens by using dual-channel confocal fluorescence microscopy. Localization of AP2 (*Left*), GluR1 (*Center*), and a merged image (*Right*) are shown (examples of colocalized puncta are indicated by arrowheads). (*B*) Hypertonic medium (350 mM sucrose) blocks AMPAR internalization. Cultures were equilibrated either in normal medium (*Left* and *Center*) or in hypertonic medium containing 350 mM sucrose (*Right*) before antibody labeling and analysis of AMPAR internalization. AMPA (100 μM, 15 min) caused clear AMPAR internalization in cells incubated in normal medium (compared *Left* and *Center*) but had minimal effects on cells preequilibrated in hypertonic medium. (*C*) Quantitation of the effect of hypertonic medium on AMPAR internalization (n = 30 for each group).

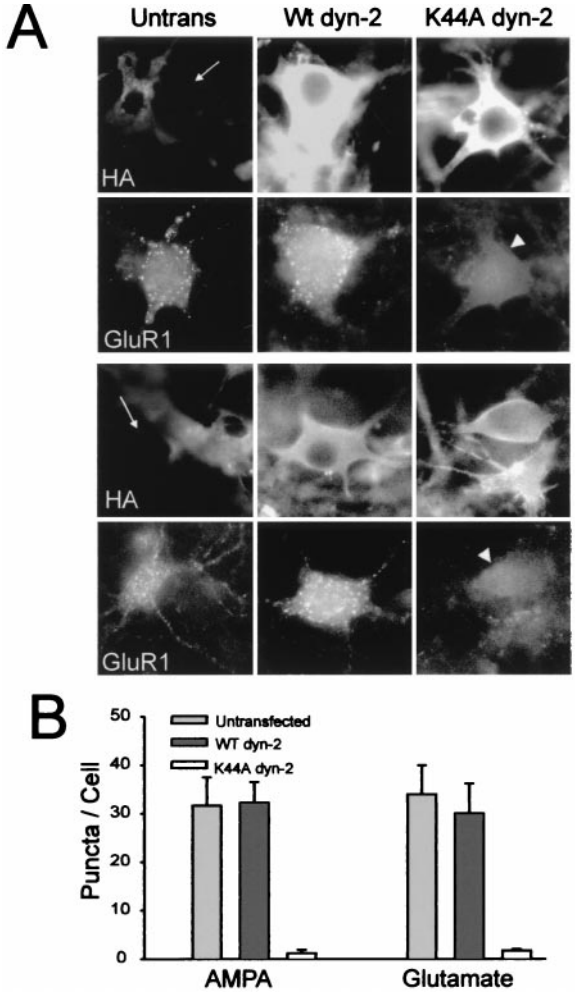

Fig. 6. Ligand-induced internalization of AMPARs is dynamin-dependent. HA-tagged wild-type or K44A mutant dynamin−2 were expressed in hippocampal cells via adenovirus-mediated transfection. Neurons were then examined for AMPAR internalization. (*A*) Micrographs showing the specific inhibition of AMPAR internalization caused by K44A mutant dynamin. The top two rows illustrate cells in which AMPAR internalization was induced by 100 μM AMPA for 15 min, conditions that induce NMDAR-independent internalization of AMPARs. The bottom two rows illustrate the same experiment conducted with the pulse–chase protocol with 10 μM glutamate applied for 1 min, conditions that reveal NMDAR-dependent internalization of AMPARs. In each set of panels, expression of HA-tagged dynamin constructs is indicated (HA), and internalized AMPARs detected in the same cells are shown (GluR1). With either protocol, substantial internalization of AMPARs was observed in cells not expressing mutant dynamin (*Left*, Untrans; arrow indicates neuron that has no detectable HA-tagged dynamin expression) or in neurons expressing HA-tagged wild-type dynamin−2 (*Center*, Wt dyn-2). In contrast, in cells expressing K44A mutant dynamin−2 (*Right*, K44A dyn-2, arrowhead), internalization of AMPARs was strongly inhibited. (*B*) Quantitation of AMPAR internalization induced by both ligand-activation protocols (n = 8 for AMPA application and n = 15 for glutamate application).

removed nearly all bound antibodies from unstimulated cells (Fig. 1*B Left* and *Center*), confirming the efficiency of this method and showing that relatively little endocytosis of receptors occurred under these conditions. In contrast, in cells incubated in the presence of AMPA (100 μM for 15 min), numerous acid-resistant puncta representing endocytic vesicles containing antibody-labeled AMPARs were observed (Fig. 1*B Right*). This internalization of AMPARs was confirmed in multiple specimens examined in a blinded manner (Fig. 1*C*; control, n = 48; AMPA, n = 48) and was prevented by the AMPAR antagonist CNQX (100 μM; n = 21).

Internalization of antibody-labeled AMPARs was first detected by the acid-stripping assay ≈5 min after application of AMPA (Fig. 2*A*). However, a pulse–chase protocol, in which short pulses (1–5 min) of AMPA were followed by AMPA washout and further incubation in the presence of CNQX, indicated that AMPAR internalization could be initiated by a significantly shorter pulse of receptor activation and could then proceed over a longer period of time in the absence of agonist (Fig. 2*B*).

An NMDAR-Dependent Component of Regulated AMPAR Endocytosis. AMPAR internalization induced by high doses of AMPA and glutamate occurred in the presence of the NMDAR antagonist D-APV (50 μM; ref. 13), indicating that this process does not require NMDAR activation. Exposure of cells to a lower dose of glutamate (10 μM) for 1 min also stimulated pronounced internalization of AMPARs (Fig. 3*A*, compare *Top* and *Middle*). Interestingly, however, the AMPAR internalization induced by this manipulation was inhibited strongly by D-APV (Fig. 3*A Bottom*). The inhibitory effect of D-APV on AMPAR internalization observed under these conditions was confirmed in multiple cells from four independent experiments (Fig. 3*B* Control, 10 μM Glutamate, and Glutamate + APV; n = 25 each).

To examine whether synaptically released glutamate could also cause AMPAR internalization, we applied KCl (30 mM for 1 min), which promotes glutamate release by depolarizing neurons (20, 21). This manipulation elicited rapid internalization of AMPARs similar to that induced by bath application of agonist

(Fig. 4*A*, compare top two panels). This KCl-induced AMPAR internalization was strongly inhibited not only by CNQX and D-APV (Fig. 4*A*, third panel) but also by D-APV alone (Fig. 4*A Bottom*), suggesting that NMDAR activation plays an important role in promoting AMPAR endocytosis in response to synaptically released glutamate. Again, these observations were confirmed in multiple cells from four independent experiments (Fig. 4*B*, $n = 23$ for each condition).

AMPAR Internalization Is Mediated by Clathrin-Coated Pits. Significant colocalization between surface-labeled AMPARs and endocytic clathrin coats labeled by an antibody to AP2 (22–24) was observed after brief (4 min at 37°C) incubation of neurons with agonist (Fig. 5*A*), suggesting that clathrin-coated pits may mediate endocytosis of AMPARs. Consistent with this hypothesis, AMPAR internalization was strongly inhibited by hypertonic conditions (350 mM sucrose; Fig. 5 *B* and *C*) that impair clathrin-mediated endocytosis (16). These conditions also strongly inhibited endocytosis of transferrin receptors in the hippocampal cultures (not shown), a process that is mediated by clathrin-coated pits (25).

Although these results are consistent with the hypothesis that AMPARs are endocytosed by clathrin-coated pits, hypertonicity has multiple cellular effects (26, 27). Therefore, we also examined the effects of K44A dynamin, a dominant-negative form of dynamin that inhibits endocytosis by clathrin-coated pits (27–29). Overexpression of K44A dynamin-2 by adenovirus-mediated gene transfer strongly inhibited internalization of AMPARs induced by 100 μM AMPA (Fig. 6*A Right*, top two rows). In contrast, AMPAR internalization was not blocked in cells overexpressing wild-type dynamin-2 at similar levels or in adjacent cells in the same field not expressing mutant dynamin (Fig. 6*A Center* and *Left*, respectively, top two rows). Similarly, internalization of AMPARs induced by 10 μM glutamate also was inhibited strongly by K44A mutant dynamin-2 (Fig. 6*A Right*, bottom two rows) but not by overexpression of wild-type dynamin-2 at similar levels (Fig. 6*A Center*, bottom two rows). These observations were confirmed in multiple experiments (Fig. 6*B*; $n = 8$ for each condition for AMPA application; $n = 15$ for each condition for glutamate application), suggesting that AMPAR internalization, induced under both NMDAR-dependent and NMDAR-independent conditions, is mediated by dynamin-dependent endocytosis of clathrin-coated pits.

Discussion

The present studies show that AMPARs can be removed from the postsynaptic plasma membrane by rapid ligand-induced endocytosis. Although various other classes of signaling receptor (e.g., receptor tyrosine kinases and G protein-coupled receptors) undergo ligand-induced endocytosis via clathrin-coated pits, to our knowledge, the present results constitute the first direct evidence that ligand-gated ion channels can be regulated in this manner. As suggested previously (13), we found that endocytosis of AMPARs was induced by high concentrations of AMPA in the absence of NMDAR activation. However, endocytosis induced by lower concentrations of glutamate or by synaptically released glutamate was inhibited strongly by D-APV, indicating an important role for NMDAR activation in initiating this process. This observation is of particular interest because of the important role of NMDARs in triggering various forms of synaptic plasticity such as long-term depression (12, 30). Our experiments also show that both NMDAR-independent and NMDAR-dependent components of AMPAR internalization are mediated by a similar, dynamin-dependent mechanism. One plausible explanation for this observation is that NMDAR-dependent increases in local calcium concentration may stimulate endocytic machinery in the postsynaptic neuron in a manner similar to the calcium-dependent regulation of endocytosis of synaptic vesicles at the presynaptic membrane (31).

Although dynamin-dependent endocytosis clearly plays a critical role in synaptic vesicle membrane recycling in the presynaptic neuron (31–33), the postsynaptic membrane has been considered a rather static structure in which receptors are stably associated with a meshwork of postsynaptic density proteins. The present observations suggest that the postsynaptic membrane, like the presynaptic membrane, is a highly dynamic structure whose biochemical composition is controlled on a rapid time scale by regulated endocytosis. Taken together with previous studies that show rapid regulation of AMPAR localization (11–13), these observations suggest that endocytic membrane trafficking in the postsynaptic neuron may play an important role in the activity-dependent modulation of synaptic strength.

We thank Sue Giller and Mark Bunin for preparation of cultures, Frances Brodsky for providing AP.6 antibody, Nigel Bunnett for use of the confocal microscope, and Steve Hardy and Dan Kalman for advice on adenovirus methods. These studies were supported by grants from the National Institutes of Health (to R.A.N., R.C.M., and M.v.Z.). R.C.M. is also supported by the Human Frontier Science Program and the McKnight Endowment Fund for Neuroscience. R.A.N. is also supported by a grant from Bristol-Myers Squibb and is a member of the Keck Center for Integrative Neuroscience and the Silvio Conte Center for Neuroscience Research.

1. Hollmann, M. & Heinemann, S. (1994) *Annu. Rev. Neurosci.* **17,** 31–108.
2. O'Brien, R. J., Lau, L. F. & Huganir, R. L. (1998) *Curr. Opin. Neurobiol.* **8,** 364–369.
3. Seeburg, P. H. (1993) *Trends Neurosci.* **16,** 359–365.
4. Gomperts, S. N., Rao, A., Craig, A. M., Malenka, R. C. & Nicoll, R. A. (1998) *Neuron* **21,** 1443–1451.
5. Malenka, R. C. & Nicoll, R. A. (1997) *Neuron* **19,** 473–476.
6. Nusser, Z., Lujan, R., Laube, G., Roberts, J. D., Molnar, E. & Somogyi, P. (1998) *Neuron* **21,** 545–559.
7. Petralia, R. S., Esteban, J. A., Wang, Y. X., Partridge, J. G., Zhao, H. M., Wenthold, R. J. & Malinow, R. (1999) *Nat. Neurosci.* **2,** 31–36.
8. Takumi, S., Ramírez-León, V., Laake, P., Rinvik, E. & Ottersen, O. (1999) *Nat. Neurosci.* **2,** 618–624.
9. Lissin, D. V., Gomperts, S. N., Carroll, R. C., Christine, C. C., Kalman, D., Kitamura, M., Hardy, S., Nicoll, R. A., Malenka, R. C. & von Zastrow, M. (1998) *Proc. Natl. Acad. Sci. USA* **12,** 7097–7102.
10. Rao, A. & Craig, A. M. (1997) *Neuron* **19,** 801–812.
11. Shi, S. H., Hayashi, Y., Petralia, R. S., Zaman, S. H., Wenthold, R. J., Svoboda, K. & Malinow, R. (1999) *Science* **284,** 1811–1816.
12. Carroll, R. C., Lissin, D. V., von Zastrow, M., Nicoll, R. A. & Malenka, R. C. (1999) *Nat. Neurosci.* **2,** 454–460.
13. Lissin, D. V., Carroll, R. C., Nicoll, R. A., Malenka, R. C. & von Zastrow, M. (1999) *J. Neurosci.* **19,** 1263–1272.
14. Wilde, A., Beattie, E. C., Lem, L., Riethof, D. A., Liu, S. H., Mobley, W. C., Soriano, P. & Brodsky, F. M. (1999) *Cell* **96,** 677–687.
15. Zhou, J., Valletta, J. S., Grimes, M. L. & Mobley, W. C. (1995) *J. Neurochem.* **65,** 1146–1156.
16. Heuser, J. E. & Anderson, R. G. (1989) *J. Cell Biol.* **108,** 389–400.
17. Altschuler, Y., Barbas, S. M., Terlecky, L. J., Tang, K., Hardy, S., Mostov, K. E. & Schmid, S. L. (1998) *J. Cell Biol.* **143,** 1871–1881.
18. von Zastrow, M. & Kobilka, B. K. (1994) *J. Biol. Chem.* **269,** 18448–18452.
19. Gruenberg, J. & Maxfield, F. R. (1995) *Curr. Opin. Cell Biol.* **7,** 552–563.
20. Betz, W. J. & Angleson, J. K. (1998) *Annu. Rev. Physiol.* **60,** 347–363.
21. Kraszewski, K., Mundigl, O., Daniell, L., Verderio, C., Matteoli, M. & De Camilli, P. (1995) *J. Neurosci.* **15,** 4328–4342.
22. Robinson, M. S. (1987) *J. Cell Sci.* **87,** 203–204.
23. Pearse, B. M. & Robinson, M. S. (1990) *Annu. Rev. Cell Biol.* **6,** 151–171.
24. Schmid, S. L. & Damke, H. (1995) *FASEB J.* **9,** 1445–1453.
25. Trowbridge, I. S., Newman, R. A., Domingo, D. L. & Sauvage, C. (1984) *Biochem. Pharmacol.* **33,** 925–932.

26. Rosenmund, C. & Stevens, C. F. (1996) *Neuron* **16,** 1197–1207.
27. Damke, H., Baba, T., Warnock, D. E. & Schmid, S. L. (1994) *J. Cell Biol.* **127,** 915–934.
28. Herskovits, J. S., Burgess, C. C., Obar, R. A. & Vallee, R. B. (1993) *J. Cell Biol.* **122,** 565–578.
29. van der Bliek, A. M., Redelmeier, T. E., Damke, H., Tisdale, E. J., Meyerowitz, E. M. & Schmid, S. L. (1993) *J. Cell Biol.* **122,** 553–563.
30. Malenka, R. C. (1994) *Cell* **78,** 535–538.
31. Cremona, O. & De Camilli, P. (1997) *Curr. Opin. Neurobiol.* **7,** 323–330.
32. Poodry, C. A. (1990) *Dev. Biol.* **138,** 464–472.
33. van der Bliek, A. M. & Meyerowitz, E. M. (1991) *Nature (London)* **351,** 411–414.